Coupling between shear and bending in the analysis of beam problems: planar case

Ahmed A. Shabana (shabana@uic.edu)
Mohil Patel (mpate72@uic.edu)

Department of Mechanical and Industrial Engineering
University of Illinois at Chicago
842 West Taylor Street
Chicago, IL 60607, U.S.A.

ABSTRACT

The interpretation of invariants, such as curvatures which uniquely define the bending and twist of space curves and surfaces, is fundamental in the formulation of the beam and plate elastic forces. Accurate representations of curve and surface invariants, which enter into the definition of the strain energy equations, is particularly important in the case of large displacement analysis. This paper discusses this important subject in view of the fact that shear and bending are independent modes of deformation and do not have kinematic coupling; this is despite the fact that kinetic coupling may exist. The paper shows, using simple examples, that shear without bending and bending without shear at an arbitrary point and along a certain direction are scenarios that higher-order finite elements (FE) can represent with a degree of accuracy that depends on the order of interpolation and/or mesh size. The FE representation of these two kinematically uncoupled modes of deformation is evaluated in order to examine the effect of the order of the polynomial interpolation on the accuracy of representing these two independent modes. It is also shown in this paper that not all the curvature vectors contribute to bending deformation. In view of the conclusions drawn from the analysis of simple beam problems, the *material curvature* used in several previous investigations is evaluated both analytically and numerically. The problems associated with the material curvature matrix, obtained using the rotation of the beam cross-section, and the fundamental differences between this material curvature matrix and the Serret-Frenet curvature matrix are discussed.

Keywords: shear deformation; bending deformation; absolute nodal coordinate formulation; finite element; large displacement.

1. Introduction

The formulation of the continuum elastic forces using a general continuum mechanics approach requires having a complete set of position vector gradients in order to properly define the components of the Green-Lagrange strain tensor or any other general strain measure [1 – 3]. Having a complete set of position vector gradients requires a full-parameterization of the continuum; two parameters for planar surfaces, and three parameters for volumes. The use of the general continuum mechanics approach in the case of fully-parameterized continuum does not require explicit definition of geometric invariants such as curvature and torsion which uniquely define the geometries of curves and surfaces [4 – 7].

When gradient deficient continuum models are used, on the other hand, the general continuum mechanics approach cannot be used. In this case, specialized classical beam and plate theories are used to formulate the stress forces [8 – 12]. In these specialized theories, the geometric invariants, such as curvature and torsion, are often used in the formulation of the energy expressions. Accurate definitions of these invariants, therefore, is necessary in order to obtain reliable solutions. A fiber of a beam, for example, can be considered as a space curve that can experience arbitrary bending deformations. The curvature of the fiber is defined as the magnitude of the curvature vector obtained by differentiation of the unit tangent with respect to the arc length. The curvature, often in a simplified form, has been widely used in the literature in the formulation of the bending strain energy [8 – 12].

In the general theory of continuum mechanics, an infinitesimal volume has six independent modes of deformation; three stretch modes and three shear modes. Simplifying assumptions are used in the development of existing beam theories which are based, for the most part, on one-dimensional parameterization. For example, in most existing beam formulations, the beam cross

section is assumed to remain planar and rigid. In the case of shear-deformable planar beams, for example, the shear is defined in terms of the angle between the beam cross section and the normal to the beam centerline. The shear angle is assumed to be totally independent from the beam bending; a beam, at an arbitrary point and along a certain direction, can bend without shear and can shear without bending. This basic assumption, which has been used for decades in the formulation of the beam equations, is also consistent with the general continuum mechanics theory in which pure shear deformation can be achieved independently from all other deformation types. The phrase "pure shear" will be used in this paper to refer to the case in which shear is the only mode of deformation experienced by the continuum. Nonetheless, in some investigations, new curvature definitions that kinematically couple the curvature and shear were introduced [13 – 15]. In some of these definitions, the angles that define the orientation of the beam cross section are used in the definition of the curvatures. A transformation matrix expressed in terms of these cross section angles is used in a manner that resembles the Serret-Frenet frame transformation used to define the curvature and torsion of a space curve [5, 6]. In the Serret-Frenet approach, the tangent, normal, and bi-normal vectors are used to define the Frenet frame which depends only on and can be uniquely defined using one parameter; the curve *arc length*.

When using the first and second fundamental theorems of surfaces [5, 6], it is important to recognize that not all curvature vectors are associated with bending deformations. Curvature vectors that involve differentiation twice with respect to the same coordinate line describe the change of the orientation of tangent vectors to fibers and can be associated with bending deformation as will be discussed in this paper. Curvature vectors that result from the differentiation with respect to two different coordinate lines (parameters) can appear in the formulation of the shear as will be demonstrated in this paper.

The absolute nodal coordinate formulation (ANCF) fully-parameterized elements allow for developing new and more general beam models and for investigating the assumptions used in the classical beam and plate theories [16 – 29]. The use of the position vector gradients as nodal coordinates allows for relaxing the assumptions of small deformation used for most conventional beam and plate elements [30 – 32]. ANCF position gradient vectors capture accurately arbitrarily large rigid body rotations and high speed spinning motion [33 – 35]. For this reason, such general elements are suited for evaluating the assumptions used in the classical approaches.

This study, which is concerned with the interpretation of the geometric invariants such as the curvature in the FE large displacement analysis, is motivated by the fact that the definition of curve and surface invariants is fundamental for the accurate beam and plate stress force formulation. The focus in this paper will be on the analysis of planar beams in order to avoid the complexities of the three-dimensional analysis and to be able to obtain simple expressions that can shed light clearly on different geometric definitions. The specific contributions of this paper can be summarized as follows:

1. It is demonstrated analytically, in Section 2, that the position vector gradients can be used to represent the case of shear without bending. To this end, each of the gradient vector is defined in terms of a stretch coefficient and an angle that defines the orientation of the gradient vector. It is shown that in the case of shear, the transverse gradient vector can have an arbitrary orientation with respect to the normal to the beam fiber. The shear can be non-uniform, while the beam fiber remains straight, demonstrating that bending cannot be defined in terms of the derivative of the shear angle.
2. In Section 3, the accuracy of using the FE approximation in the representation of the shear without bending (SWB) and bending without shear (BWS) is examined. To this end, a fully-

parameterized ANCF beam element is used to formulate the beam problem [20]. It is shown that higher-order elements can be used systematically to obtain the SWB and BWS scenarios in the case of arbitrarily large rigid body displacement.

3. It is shown in Section 4 that a curvature vector obtained by differentiation with respect to two different coordinate lines (parameters) may not be associated with bending deformation, and such a curvature vector can appear in the formulation of the SWB problem. This curvature vector can be related to the derivative of the angle that defines the orientation of the cross section with respect to the arc length parameter.
4. Based on the conclusions drawn from the analysis presented in Sections 2 and 3, the definition of the *material curvature* used by other researchers is evaluated in Section 4 [13 – 15]. Despite the fact that the material curvature is defined in terms of the angle that defines the orientation of the beam cross section, the material curvature was used by some researchers to formulate the beam bending forces.
5. The fundamental differences between the Serret-Frenet approach and the material curvature approach that employs the cross section orientation matrix, are highlighted in Section 4 of the paper.
6. Simple numerical examples are used throughout the paper to examine the effect of the FE interpolation in the representation of the SWB and BWS cases. Simple numerical examples are also used in Section 5 to evaluate the definition of the material curvature matrix.
7. The new analytical and numerical results obtained in this paper clearly show that the definition of the material curvature can lead to wrong results when the shear deformation is dominant, and the material curvature converges to the differential geometry-based curvature only when the shear deformation is not considered.

2. Generalized shear forces

The shear angle in the simple planar analysis is defined as the angle between the normal to the beam centerline and the beam cross-section. This angle, therefore, is independent of the angle that defines the orientation of the normal or the tangent to the centerline. In the planar analysis, the matrix that defines the Frenet frame in differential geometry is formed using the unit tangent and unit curvature (normal) vectors. The change of the orientation of the tangent to a curve such as the beam centerline defines the bending or the curvature of the curve; the curvature is defined to be the norm of the curvature vector which is obtained by differentiating the unit tangent with respect the arc length of the curve.

2.1 *Alternate position vector gradient representation*

In order to develop expressions for the generalized shear forces, the position gradient vectors that enter into the definition of the Green-Lagrange strains are written in this section using a stretch coefficient and an angle that defines the orientation of the gradient vector. While this representation preserves the generality of the analysis because it allows for a change in the magnitude and orientation of the position vector gradients, it provides a convenient way for obtaining the deformation modes that will be discussed in this paper. Each of the position vector gradients can be written in terms of a stretch coefficient and a unit vector as

$$\mathbf{r}_x = \alpha_x \left[\cos\beta_x \quad \sin\beta_x\right]^T, \quad \mathbf{r}_y = \alpha_y \left[-\sin\beta_y \quad \cos\beta_y\right]^T \tag{1}$$

In this equation, $\alpha_x = \alpha_x\left(x,y,t\right)$ and $\alpha_y = \alpha_y\left(x,y,t\right)$ are stretch coefficients, and $\beta_x = \beta_x\left(x,y,t\right)$ and $\beta_y = \beta_y\left(x,y,t\right)$ are angles that define the orientations of the gradient vectors. In this investigation, it is assumed that β_x and β_y are not, in general, the same in order to allow for shear

deformations. If the condition $\alpha_y = 1$ is enforced, the stretch of the cross section is not allowed. The dependence of α_x on y allows for accounting for the effect of bending when a general continuum mechanics approach is used to formulate the elastic forces. The assumption $\alpha_y = 1$ will be used in some sections of this paper in order to focus on the shear deformation and develop models that employ some of the basic assumptions used in the classical beam formulations.

The components of the Green-Lagrangian strain tensor can be written in terms of these position vector gradients as

$$\left.\begin{aligned} \varepsilon_{11} &= \frac{1}{2}\left(\mathbf{r}_x^T\mathbf{r}_x - 1\right) = \frac{1}{2}\left(\alpha_x^2 - 1\right), \\ \varepsilon_{22} &= \frac{1}{2}\left(\mathbf{r}_y^T\mathbf{r}_y - 1\right) = \frac{1}{2}\left(\alpha_y^2 - 1\right), \\ \varepsilon_{12} &= \frac{1}{2}\mathbf{r}_x^T\mathbf{r}_y = \frac{1}{2}\alpha_x\alpha_y \sin\left(\beta_x - \beta_y\right) \end{aligned}\right\} \tag{2}$$

Using the stretch coefficient and the angle representation for the gradient vectors, it is clear from the above equation that the components of the Green-Lagrange strain tensor are written in terms of two stretch coefficients and one angle $\left(\beta_y - \beta_x\right)$ which defines the shear angle. It is also clear that if the gradient vectors are not orthogonal, the stretch coefficients α_x and α_y contribute to the shear strain. It follows that a virtual change in the strain components can be written in terms of the virtual change of the stretch coefficients and the angles as

$$\left.\begin{aligned} &\delta\varepsilon_{11} = \mathbf{r}_x^T\delta\mathbf{r}_x = \alpha_x\delta\alpha_x, \qquad \delta\varepsilon_{22} = \mathbf{r}_y^T\delta\mathbf{r}_y = \alpha_y\delta\alpha_y \\ &\delta\varepsilon_{12} = \frac{1}{2}\left(\mathbf{r}_y^T\delta\mathbf{r}_x + \mathbf{r}_x^T\delta\mathbf{r}_y\right) = -\frac{1}{2}\left(\left(\sin\gamma\right)\left(\alpha_y\delta\alpha_x + \alpha_x\delta\alpha_y\right) + \alpha_x\alpha_y\left(\cos\gamma\right)\left(\delta\gamma\right)\right) \end{aligned}\right\} \tag{3}$$

In this equation, $\gamma = \beta_y - \beta_x$ is the shear angle. It is important, however, to note that the shear strain does not depend only on this shear angle, and therefore, using this angle to formulate the shear strain energy should be viewed as an approximation. Careful examination of the virtual

changes of Eq. 3 sheds light on the generalized elastic forces that will be developed in terms of the stretch coefficients and the angles that define the orientations of the position vector gradients.

2.2 *Planar rigid cross section*

If the condition $\alpha_y = 1$, that is no cross section stretch, is enforced and warping of the beam cross section is not considered, the virtual change in the strain components reduces to

$$\left.\begin{aligned} &\delta\varepsilon_{11} = \alpha_x \delta\alpha_x, \qquad \delta\varepsilon_{22} = 0 \\ &\delta\varepsilon_{12} = \frac{1}{2}\left(\mathbf{r}_y^T \delta\mathbf{r}_x + \mathbf{r}_x^T \delta\mathbf{r}_y\right) = -\frac{1}{2}\left(\left(\sin\gamma\right)\delta\alpha_x + \alpha_x\left(\cos\gamma\right)\delta\gamma\right) \end{aligned}\right\} \tag{4}$$

It is clear from this equation that the shear strain ε_{12} is function of the shear angle γ. The curvature at an arbitrary point on an arbitrary fiber of the continuum for a given y is defined as $\kappa = \partial\beta_x / \partial s$, where s is the arc length. It is important, however, to point out that, in general, there is no relationship between $\partial\beta_x / \partial s$ and $\partial\beta_y / \partial s$. This important issue will be revisited when discussing the material curvature in a later section of this paper. Using the form of the position vector gradients introduced in this section, it is clear that the curvature of a fiber for a given y does not depend on the stretch coefficient α_x. This is clear from the fact that the derivative of the unit tangent (gradient) vector $\hat{\mathbf{r}}_x = \left[\cos\beta_x \quad \sin\beta_x\right]^T$ with respect to the arc length defines the curvature vector $\partial\hat{\mathbf{r}}_x / \partial s = \left(\partial\beta_x / \partial s\right)\left[-\sin\beta_x \quad \cos\beta_x\right]^T$, demonstrating that the magnitude of the curvature vector is $\partial\beta_x / \partial s$ regardless of the change in the stretch coefficient α_x.

2.3 *Shear deformation without bending*

In the case of shear without bending (SWB), $\alpha_x = 1$ and $\delta\alpha_x = 0$. In this special case, one has $\delta\varepsilon_{11} = 0, \delta\varepsilon_{22} = 0, \delta\varepsilon_{12} = -\left(\cos\gamma\right)\delta\gamma / 2$. The virtual work of the elastic forces in this special case

reduces to $\delta W_s = -2\int_V \sigma_{12}\delta\varepsilon_{12}dV$, where $\sigma_{12} = 2G\varepsilon_{12}$ is the shear stress, G is the modulus of rigidity, and V is the continuum volume. It follows that

$$\begin{aligned}\delta W_s &= -2\int_V \sigma_{12}\delta\varepsilon_{12}dV = -2\int_V \left(-G\sin\gamma\right)\left(-\frac{1}{2}\left(\cos\gamma\right)\delta\gamma\right)dV \\ &= -\frac{G}{2}\int_V \left(\sin 2\gamma\right)\delta\gamma dV\end{aligned} \tag{5}$$

The virtual change $\delta\gamma$ can be expressed in terms of the virtual change in the coordinates used to define the continuum configuration. For example, if the method of separation of variable is used to write the position vector $\mathbf{r}$ as $\mathbf{r}\left(x,y,t\right) = \mathbf{S}\left(x,y\right)\mathbf{e}\left(t\right)$, where $\mathbf{S}$ is a shape matrix that depends on the spatial coordinates and $\mathbf{e}$ is the vector of time dependent coordinates, then a virtual change in the position and gradient coordinates can be written as $\delta\mathbf{r} = \mathbf{S}\delta\mathbf{e}$, $\delta\mathbf{r}_x = \left[\mathbf{S}_{1x}^T \quad \mathbf{S}_{2x}^T\right]^T\delta\mathbf{e}$, and $\delta\mathbf{r}_y = \left[\mathbf{S}_{1y}^T \quad \mathbf{S}_{2y}^T\right]^T\delta\mathbf{e}$, where $\mathbf{S}_{jk}$, $j = 1,2$, $k = x,y$ is the partial derivatives of row j of the shape matrix $\mathbf{S}$ with respect to the spatial coordinate k. Using these definitions, one can show that the virtual change in the shear angle γ can be written systematically in terms of the virtual change of the coordinates as $\delta\gamma = \mathbf{H}_s\left(x,y,t\right)\delta\mathbf{e}$, where $\mathbf{H}_s$ is an appropriate velocity transformation matrix. The virtual work of the elastic forces can then be written as

$$\delta W_s = -\left(\frac{G}{2}\int_V \left(\sin 2\gamma\right)\mathbf{H}_s dV\right)\delta\mathbf{e} \tag{6}$$

This equation defines generalized shear moments associated with the elastic coordinates as $M_s = -G\int_V \left(\sin 2\gamma\right)\mathbf{H}_s dV \Big/ 2$. Clearly, these generalized moment are not associated with bending deformation.

2.4 *Shear and bending*

According to the more general continuum mechanics principles and the principles of the simplified linear vibration theory, the bending and shear are independent modes of deformation and they should not be kinematically coupled. Pure shear deformation should not produce bending and should not change the curvature of the fibers. This fact, which is crucial in the discussion provided later in this paper on the material curvature, can be easily proved. Because in the SWB case considered in this paper, the axial and transverse normal strains $\varepsilon_{11} = 0$ and $\varepsilon_{22} = 0$, that is, $\mathbf{r}_x^T \mathbf{r}_x = 1$ and $\mathbf{r}_y^T \mathbf{r}_y = 1$, differentiation of the first equation with respect to y and the second equation with respect to x shows that $\mathbf{r}_{xy}^T \mathbf{r}_x = 0$ and $\mathbf{r}_{yx}^T \mathbf{r}_y = 0$, this is with the understanding that $\mathbf{r}_{yx} = \mathbf{r}_{xy}$ and the FE interpolations may not enforce these conditions everywhere within the element. These two equations show that the rate of change of a gradient vector tangent to one coordinate line with respect to the other coordinate line is zero along the other tangent vector, demonstrating that the fibers at a point and along a certain direction can rotate without bending as shown in Fig. 1. Therefore, the shear without bending is associated with a rotation that does not contribute to the bending deformation at a point along a certain direction. Nonetheless, if the two gradient vectors $\mathbf{r}_x$ and $\mathbf{r}_y$ are not orthogonal, a change in the length of these vectors without a change in the shear angle can also lead to a change in the shear strain as it is clear from the definition $\varepsilon_{12} = (1/2)\mathbf{r}_x^T \mathbf{r}_y$. That is, the shear, in the general theory of continuum mechanics, cannot be described completely by an angle.

3. Finite element discretization

The position field of the planar ANCF shear deformable beam element used in this investigation can be written as [20]

$$\mathbf{r}(x,y,t)=\bar{\mathbf{r}}(x,t)+y\mathbf{r}_y(x,t) \tag{7}$$

In this equation, x and y are, respectively, the longitudinal and transverse spatial coordinates of the element, $\bar{\mathbf{r}}=\mathbf{r}(y=0)$ is the position vector of an arbitrary point on the beam centerline, and $\mathbf{r}_y=\partial\mathbf{r}/\partial y$ is the transverse position gradient vector. Using the shape functions presented in the appendix of this paper, one can show that, for this particular element, a linear interpolation is used for $\mathbf{r}_y$ and such an interpolation is defined in terms of the nodal transverse position gradient vectors as $\mathbf{r}_y=(1-\xi)\mathbf{r}_y^1+\xi\mathbf{r}_y^2$, where $\xi=x/l$, l is the length of the element, and superscript $k=1,2$ refers to the node number. Furthermore, the shape functions presented in the appendix show that $\bar{\mathbf{r}}=\mathbf{r}(y=0)$ does not depend on the transverse gradient vectors at the nodes. It follows that the position gradient vector associated with the axial coordinate x can be written as $\mathbf{r}_x=\bar{\mathbf{r}}_x+y\mathbf{r}_{xy}$.

3.1 *Shear without bending*

The higher-order ANCF planar beam element allows for creating easily different deformation scenarios that will shed light on the fundamental issues considered in this investigation [20]. For example, a shear deformation without bending can be described by the following vector of nodal coordinates:

$$\begin{aligned}\mathbf{e}=\big[&x_1 \quad y_1 \quad \cos\theta \quad \sin\theta \quad -\sin(\theta+\gamma_1) \quad \cos(\theta+\gamma_1)\\ &(x_1+l\cos\theta) \quad (y_1+l\sin\theta) \quad \cos\theta \quad \sin\theta \quad -\sin(\theta+\gamma_2) \quad \cos(\theta+\gamma_2)\big]^T\end{aligned} \tag{8}$$

In this equation, x_1 and y_1 represent an arbitrary rigid body translation, θ is an arbitrary rigid body rotation, and γ_1 and γ_2 are shear angles at the first and second nodes, respectively. Using this vector of nodal coordinates and the shape functions presented in the appendix, one can show

that the position, gradient, and curvature vectors at an arbitrary point on the element can be written as

$$\left.\begin{aligned}
\mathbf{r} &= \begin{bmatrix} x_1 \\ y_1 \end{bmatrix} + \xi l \begin{bmatrix} \cos\theta \\ \sin\theta \end{bmatrix} + \eta l \left((1-\xi) \begin{bmatrix} -\sin(\theta+\gamma_1) \\ \cos(\theta+\gamma_1) \end{bmatrix} + \xi \begin{bmatrix} -\sin(\theta+\gamma_2) \\ \cos(\theta+\gamma_2) \end{bmatrix} \right) \\
\mathbf{r}_x &= \begin{bmatrix} \cos\theta \\ \sin\theta \end{bmatrix} + \eta \begin{bmatrix} \sin(\theta+\gamma_1) - \sin(\theta+\gamma_2) \\ -\cos(\theta+\gamma_1) + \cos(\theta+\gamma_2) \end{bmatrix} \\
\mathbf{r}_y &= (1-\xi) \begin{bmatrix} -\sin(\theta+\gamma_1) \\ \cos(\theta+\gamma_1) \end{bmatrix} + \xi \begin{bmatrix} -\sin(\theta+\gamma_2) \\ \cos(\theta+\gamma_2) \end{bmatrix} \\
\mathbf{r}_{xy} &= \frac{1}{l} \begin{bmatrix} \sin(\theta+\gamma_1) - \sin(\theta+\gamma_2) \\ -\cos(\theta+\gamma_1) + \cos(\theta+\gamma_2) \end{bmatrix}
\end{aligned}\right\} \tag{9}$$

In this equation, $\eta = y/l$. The configuration of the beam in this special SWB case is shown in Fig. 2 in the case of zero rigid body motion, that is, $x_1 = y_1 = \theta = 0$, and for the shear angles $\gamma_1 = 45°$ and $\gamma_2 = -45°$. The preceding equation shows that for a given η, the position gradient vector $\mathbf{r}_x$ assumes a constant orientation within the element, demonstrating the fact that the shear does not produce bending of the longitudinal fibers of the beam. Similarly for a given value of ξ, the position vector gradient vector $\mathbf{r}_y$ assumes a constant orientation within the element, demonstrating that the shear deformation does not produce bending of the transverse fibers. This fact is demonstrated clearly in Fig. 1. It is also important to understand that the curvature vector $\mathbf{r}_{xy}$ in the SWB case is not associated with bending of fibers; it describes the change of the orientation of the gradient vector $\mathbf{r}_x$ as y is changed and describes the change of the orientation of $\mathbf{r}_y$ as x is changed. This fact is also clear from Fig. 1. It is clear, therefore, that in the SWB case, the fibers may change their orientation, but they do not bend since shear is an independent deformation mode; this is despite the fact that there can be force coupling between these two modes of deformation.

3.2 *Finite element approximation*

If the shear angle within the element is such that $\gamma_1 \approx \gamma_2$, a condition that can be ensured if the element length or the shear angle is small, one obtains

$$\mathbf{r}_x \approx \begin{bmatrix} \cos\theta \\ \sin\theta \end{bmatrix}, \quad \mathbf{r}_y \approx \begin{bmatrix} -\sin(\theta+\gamma_1) \\ \cos(\theta+\gamma_1) \end{bmatrix}, \quad \mathbf{r}_{xy} \approx \mathbf{0} \tag{10}$$

In this case,

$$\varepsilon_{11} = \frac{1}{2}\left(\mathbf{r}_x^T\mathbf{r}_x - 1\right) = 0, \quad \varepsilon_{22} = \frac{1}{2}\left(\mathbf{r}_y^T\mathbf{r}_y - 1\right) = 0, \quad \varepsilon_{12} = \frac{1}{2}\mathbf{r}_x^T\mathbf{r}_y = -\frac{1}{2}\sin\gamma_1 \tag{11}$$

Using the equations presented in this section, one can show that in the case of pure shear, the normal strains at the nodes are identically equal to zero.

3.3 *Bending deformation*

The special case of bending without shear (BWS) can be described by the following vector of ANCF nodal coordinates:

$$\begin{aligned} \mathbf{e} = \big[& x_1 \quad y_1 \quad \cos(\theta+\beta_1) \quad \sin(\theta+\beta_1) \quad -\sin(\theta+\beta_1) \quad \cos(\theta+\beta_1) \\ & (x_1 + l\cos\theta) \quad (y_1 + l\sin\theta) \quad \cos(\theta+\beta_2) \quad \sin(\theta+\beta_2) \quad -\sin(\theta+\beta_2) \quad \cos(\theta+\beta_2) \big]^T \end{aligned} \tag{12}$$

Using the shape functions given in the appendix, one can show that the configuration of the beam is defined by the following equation:

$$\begin{aligned} \mathbf{r} = & \begin{bmatrix} x_1 \\ y_1 \end{bmatrix} + l\left(3\xi^2 - 2\xi^3\right)\begin{bmatrix} \cos\theta \\ \sin\theta \end{bmatrix} + l\left(\xi - 2\xi^2 + \xi^3\right)\begin{bmatrix} \cos(\theta+\beta_1) \\ \sin(\theta+\beta_1) \end{bmatrix} + \\ & l\eta(1-\xi)\begin{bmatrix} -\sin(\theta+\beta_1) \\ \cos(\theta+\beta_1) \end{bmatrix} + l\left(-\xi^2 + \xi^3\right)\begin{bmatrix} \cos(\theta+\beta_2) \\ \sin(\theta+\beta_2) \end{bmatrix} + l\xi\eta\begin{bmatrix} -\sin(\theta+\beta_2) \\ \cos(\theta+\beta_2) \end{bmatrix} \end{aligned} \tag{13}$$

Figure 3 shows the configuration of the beam for the rigid body rotation $\theta = 0°$, $\beta_1 = 45°$, and $\beta_2 = -45°$. The longitudinal position vector gradient is given in this case as

$$\begin{aligned}\mathbf{r}_x = 6\left(\xi - \xi^2\right)\begin{bmatrix}\cos\theta \\ \sin\theta\end{bmatrix} + \left(1 - 4\xi + 3\xi^2\right)\begin{bmatrix}\cos\left(\theta+\beta_1\right) \\ \sin\left(\theta+\beta_1\right)\end{bmatrix} - \\ \eta\begin{bmatrix}-\sin\left(\theta+\beta_1\right) \\ \cos\left(\theta+\beta_1\right)\end{bmatrix} + \left(-2\xi + 3\xi^2\right)\begin{bmatrix}\cos\left(\theta+\beta_2\right) \\ \sin\left(\theta+\beta_2\right)\end{bmatrix} + \eta\begin{bmatrix}-\sin\left(\theta+\beta_2\right) \\ \cos\left(\theta+\beta_2\right)\end{bmatrix}\end{aligned} \tag{14}$$

The transverse position vector gradient is given by

$$\mathbf{r}_y = \left(1-\xi\right)\begin{bmatrix}-\sin\left(\theta+\beta_1\right) \\ \cos\left(\theta+\beta_1\right)\end{bmatrix} + \xi\begin{bmatrix}-\sin\left(\theta+\beta_2\right) \\ \cos\left(\theta+\beta_2\right)\end{bmatrix} \tag{15}$$

The curvature vector $\mathbf{r}_{xy}$ is defined in this BWS case as

$$\mathbf{r}_{xy} = \frac{1}{l}\left(\mathbf{r}_y^2 - \mathbf{r}_y^1\right) = \frac{1}{l}\left(\begin{bmatrix}-\sin\left(\theta+\beta_2\right) \\ \cos\left(\theta+\beta_2\right)\end{bmatrix} - \begin{bmatrix}-\sin\left(\theta+\beta_1\right) \\ \cos\left(\theta+\beta_1\right)\end{bmatrix}\right) \tag{16}$$

Using these equations, one can show that at the nodes, in this BWS case, the shear strain $\varepsilon_{12} = \mathbf{r}_x^T\mathbf{r}_y/2$ is identically zero. Similarly, at the nodes, the normal strain $\varepsilon_{22} = \left(\mathbf{r}_y^T\mathbf{r}_y - 1\right)/2$ is identically zero. This demonstrates that in the BWS case, there is only one non-zero Green-Lagrange strain ε_{11}. In the case of symmetric bending, the centerline does not stretch, while fibers below and above the centerline, as shown in Fig. 4, shorten and elongate, respectively. This is in turn produces axial stresses that define the beam bending moment. Strains at an arbitrary points that are not nodal points can be determined using the FE interpolation. For example in the case of Euler-Bernoulli beam theory, the axial strain is zero at the beam neutral axis, while the strain is assumed to vary linearly away from the neutral axis.

3.4 *Generalized bending forces*

One can also show that the axial component of the Green-Lagrange strain tensor can be written in its most general form in the case of the ANCF element considered in this section as

$$\varepsilon_{11} = \frac{1}{2}\left(\mathbf{r}_x^T\mathbf{r}_x - 1\right) = \frac{1}{2}\left(\left(\overline{\mathbf{r}}_x^T\overline{\mathbf{r}}_x - 1\right) + 2y\overline{\mathbf{r}}_x^T\mathbf{r}_{xy} + y^2\mathbf{r}_{xy}^T\mathbf{r}_{xy}\right) \tag{17}$$

Using this definition of the axial strain, the virtual work of the generalized elastic bending forces in the case of linear elastic material can be written as

$$\delta W_s = -\int_V \sigma_{11}\delta\varepsilon_{11}dV = -\int_V E\varepsilon_{11}\delta\varepsilon_{11}dV \tag{18}$$

In this equation, E is the modulus of elasticity, and σ_{11} is the axial stress. The virtual change in ε_{11} can be systematically expressed in terms of the virtual change of the element coordinates as $\delta\varepsilon_{11} = \mathbf{H}_b\left(x,y,t\right)\delta\mathbf{e}$, where $\mathbf{H}_b$ is an appropriate velocity transformation matrix. This equation can be substituted into the virtual work expression to define the generalized bending moments associated with the element generalized coordinates.

4. Material curvature

As previously mentioned, in the continuum mechanics theory, bending and shear are independent modes of deformation and they should not be kinematically coupled. Kinetic or stiffness coupling may exist between independent modes, coordinates, or degrees of freedom. According to the principles of continuum mechanics, deformation can occur in a shear mode only or bending mode only. Fluids, for example, can be subjected to only shear forces and a solid, at an arbitrary point and along a certain direction, can deform in a shear mode only without having any other mode of deformation. A beam, at an arbitrary point and along a certain direction, can bend without shear and can shear without bending. Having a kinematic relationship between the shear and bending deformations violates these basic principles.

As also demonstrated in this paper, not all curvature vectors are associated with bending deformations. A curvature vector is associated with a bending deformation if it describes the change of the orientation of a tangent vector along the same coordinate line (fiber) used to define the tangent vector. This fact was clearly demonstrated using the planar analysis presented in this paper.

Despite the known facts and principles mentioned above, some investigations proposed bending definitions that are based on the rotation of the beam cross section. In the case of a shear deformable beam element, the rotation of the cross section with respect to the normal to the beam centerline curve defines the shear angle. Additionally, if the gradient vectors are not orthogonal, the stretch can contribute to the change in the shear strain, as previously discussed. Therefore, using derivatives of the rotations that define the orientation of the beam cross section to define curvatures that enter into the formulation of the beam bending forces implies that non-uniform shear must be accompanied by bending, which violates the fact that the shear and bending modes should not be kinematically related. The curvature of the beam fibers is defined as the magnitude of the curvature vector obtained by differentiating the unit tangent with respect to the arc length parameter. One can show that this curvature can also be defined as the derivative of the angle that defines the orientation of the tangent vector with respect to the arc length, as previously shown in the paper. One of the definitions which kinematically relate the shear to the curvature is what is referred to as the *material curvature* which will be discussed in this section.

4.1 Bending and curvature vectors

Some of the new FE formulations offer the opportunity for the evaluation of some geometric definitions that have not been evaluated before. For example, fully-parameterized ANCF beam elements can be used to develop more general beam theories that account for shear and warping.

As previously shown in this paper, one of the ANCF planar elements can be used to define three curvature vectors $\mathbf{r}_{xx}, \mathbf{r}_{yy}$, and $\mathbf{r}_{xy}$. The first two curvature vectors describe the rate of change of the orientation of tangent vectors along the two coordinate lines x and y, and therefore, they can be associated with bending deformations. The curvature vector $\mathbf{r}_{xy}$ needs to be interpreted differently since it does not define the rate of change of the orientation of a tangent vector along the same coordinate line. The meaning of the curvature vector $\mathbf{r}_{xy}$ can be further explained by writing the displacement field of the planar fully-parameterized ANCF beam element as $\mathbf{r} = \bar{\mathbf{r}} + y\mathbf{r}_y$. In this equation, $\bar{\mathbf{r}} = \mathbf{r}(y = 0)$ defines the absolute position of the material points on the beam centerline, as previously mentioned. It is clear from this equation that if $\mathbf{r}_y$ is interpolated linearly as in the case of the original fully-parameterized beam element then $\mathbf{r}_{xx} = \bar{\mathbf{r}}_{xx}$, $\mathbf{r}_{yy} = \mathbf{0}$, and $\mathbf{r}_{yx} = \partial \mathbf{r}_y / \partial x$, the latter as it was previously shown can be written in terms of the transverse gradients at the nodal points as $\mathbf{r}_{xy} = \left(\mathbf{r}_y^2 - \mathbf{r}_y^1\right)/l$. A more general expression that will shed light on some of the definitions that will be developed in this section can be obtained for the curvature vector $\mathbf{r}_{xy}$ in the case of a beam model based on the assumption of a rigid cross section. In this case, $\mathbf{r}_y$ remains a unit vector (no cross-section stretch) and $\mathbf{r}_{xx} = \mathbf{0}$, that is, the centerline of the beam does not experience any bending. In this special case, without loss of generality, one can write $\mathbf{r}_y$ in terms of an angle as $\mathbf{r}_y = \begin{bmatrix} -\sin\theta_c & \cos\theta_c \end{bmatrix}^T$, where $\theta_c = \theta_c(x)$ can have value that varies as function of the coordinate x or the arc length s. It follows that

$$\mathbf{r}_{xy} = -\theta_c' \begin{bmatrix} \cos\theta_c & \sin\theta_c \end{bmatrix}^T \tag{19}$$

where $\theta_c' = \partial\theta_c/\partial x$. The curvature vector $\mathbf{r}_{xy}$ represents the rate of change of the tangent vector $\mathbf{r}_y$ in the direction of the coordinate line x. Because $\mathbf{r}_{xy} = \mathbf{r}_{yx}$, the curvature vector $\mathbf{r}_{xy}$ also represents the rate of change of the tangent vector $\mathbf{r}_x$ in the direction of the coordinate line y. Therefore, in the simple case described in this section, the curvature vector $\mathbf{r}_{xy}$ is not associated with bending; it describes how the fibers of the beams are oriented. For example, for a given y, the change of the orientation of $\mathbf{r}_y$ as x changes will describe how the rigid fibers of the cross section are oriented. Similarly, for a given x, the change of the orientation of $\mathbf{r}_x$ as y changes describes the orientation of the fibers which were originally parallel to the beam centerline in the straight configuration. This deformation scenario is shown in Fig. 1 where several fibers along the coordinate lines x and y are shown to rotate as rigid lines that do not experience bending.

4.2 *Material curvature*

The partial differential equation that governs the bending vibration of beams is a fourth order equation defined as $\rho A\left(\partial^2 v/\partial t^2\right) + EI\left(\partial^4 v/\partial x^4\right) = F\left(x,t\right)$, where ρ is the mass density, A is the cross section area, v is the bending deformation, E is the modulus of elasticity, I is the second moment of area, and F is the forcing function. Because of the fourth derivative with respect to the axial coordinate x, classical and computational approaches assumed interpolating functions of order three (cubic) or higher. Such an approach ensures that the curvature of the beam is properly captured. A lower order of interpolation cannot be used with the fourth order beam equation to obtain a meaningful solution and capture the beam bending under more general loading conditions.

When low-order elements are used in the FE analysis, the curvature may not be defined properly. For example, if an element based on a first-order polynomial approximation is used, the curvature within the element will always be zero, and if an element based on quadratic

interpolation, the curvature within the element will be constant (circle with constant radius of curvature). This is the main reason, cubic interpolation is always used to properly capture beam bending. However, low-order elements such as rectangular, triangular, solid, and tetrahedral elements have been used in modeling beam problems. While these low-order elements do not ensure the continuity of the rotation field at the nodal points, they are often used with a general continuum mechanics approach that employs Green-Lagrange strain tensor. In this case, an explicit definition of the curvature is not necessary since the elastic forces are formulated using the stress and strain tensors with an appropriate constitutive model. Some researchers who investigated beam bending, however, suggested the use of curvature definitions that differ from the differential geometry definitions for the use with the low-order finite elements. One of these definitions is the material curvature introduced by Simo et al. [13 - 15] and used with the large rotation vector formulations (LRVF). In this definition, the matrix $\mathbf{R}$ that defines the orientation of the beam cross section is used to define a curvature matrix as $\boldsymbol{\kappa} = \mathbf{R}^T \left(\partial \mathbf{R} / \partial s \right)$. It is important to point out that the material curvature matrix $\boldsymbol{\kappa}$ is not the same as the Serret-Frenet matrix obtained from a parameterized curve. In the Serret-Frenet approach, no cross section that has independent rotation from the rigid surface normal to the tangent vector is used. In the case of planar analysis, the matrices $\mathbf{R}$ and $\partial \mathbf{R} / \partial s$ are given, respectively, by

$$\mathbf{R} = \begin{bmatrix} \cos\theta_c & -\sin\theta_c \\ \sin\theta_c & \cos\theta_c \end{bmatrix}, \quad \partial \mathbf{R} / \partial s = \theta_c' \begin{bmatrix} -\sin\theta_c & -\cos\theta_c \\ \cos\theta_c & -\sin\theta_c \end{bmatrix} \tag{20}$$

Using these general definition for the planar transformation, one can show that

$$\boldsymbol{\kappa} = \mathbf{R}^T \left(\partial \mathbf{R} / \partial s \right) = \theta_c' \begin{bmatrix} 0 & -1 \\ 1 & 0 \end{bmatrix} \tag{21}$$

It is clear that this matrix is expressed in terms of the derivative of the angle that defines the orientation of the cross section with respect to the arc length. In the case of non-uniform shear without bending, the use of the definition of the above equation to formulate the bending elastic forces may not be appropriate because bending and shear are assumed to be independent modes of deformations. It is important also to point out that in the three-dimensional case, the analysis becomes much more complicated and other deformation modes such as torsion and out-of-plane bending must be considered. In the case of shear-deformable beam, the cross section is assumed to have an independent rotation that is not kinematically related to the rotation that defines the orientation of the tangent line used in the derivation of the Serret-Frenet frame.

4.3 *Serret-Frenet matrix*

In the case of a planar curve, the Frenet frame is defined using an orthogonal matrix $\mathbf{R}_f$ whose first column is the tangent vector $\mathbf{r}_s$ and its second column is the unit curvature vector $\widehat{\mathbf{b}} = \mathbf{r}_{ss}/\kappa$, where $\kappa = |\mathbf{r}_{ss}|$, and $\mathbf{r}_{ss} = \partial \mathbf{r}_s / \partial s$, that is $\mathbf{R}_f = \begin{bmatrix} \mathbf{r}_s & \widehat{\mathbf{b}} \end{bmatrix}$. It follows that $\partial \mathbf{R}_f / \partial s = \begin{bmatrix} \mathbf{r}_{ss} & \partial \widehat{\mathbf{b}} / \partial s \end{bmatrix}$. Using the well-known orthogonality relationships between the Frenet vectors [5, 6], one can show that curvature matrix $\boldsymbol{\kappa}_f$ associated with a space curve is defined as

$$\boldsymbol{\kappa}_f = \mathbf{R}_f^T \left(\partial \mathbf{R}_f / \partial s \right) = \kappa \begin{bmatrix} 0 & -1 \\ 1 & 0 \end{bmatrix} \tag{22}$$

This matrix is obtained using the tangent vector to the space curve and it is not associated with another independent angle or a cross section. The curvature κ which appears in this matrix is obtained as $\kappa = |\mathbf{r}_{ss}|$, as previously stated.

4.4 *Summary*

In the following section, examples will be presented in order to evaluate the use of the material curvature. Before presenting such a numerical evaluation, it is necessary to summarize some important conclusions based on the simple planar analysis considered in this study:

1. In the LRVF beams, only one parameter is used to define the beam kinematics (axial coordinate x), and therefore, the discussion presented in this section on the curvature vector $\mathbf{r}_{xy}$ is not relevant to LRVF beam problems. Nonetheless, it is important to recognize that the curvature vector $\mathbf{r}_{xy}$ may not be directly related to the bending of beam fibers and may be related to the derivative of the angle that defines the orientation of the beam cross-section when more general ANCF beam elements are used.
2. It follows that the curvature vector $\mathbf{r}_{xy}$ can be a non-zero vector while no bending is experienced as shown by the results of Fig. 5. That is, in the case of a surface, the curvature vector $\mathbf{r}_{xy}$ used in the second fundamental form of surfaces should be interpreted differently from the other two curvature vectors $\mathbf{r}_{xx}$ and $\mathbf{r}_{yy}$ when discussing bending of beams and plates.
3. The analysis presented in this section shows that while $\mathbf{r}_{xy}$ is called a curvature vector, this vector is more associated with shear mode of deformation in the simple beam example considered.
4. If $\mathbf{r}_y$ is linearly interpolated as $\mathbf{r}_y = (1-\xi)\mathbf{r}_y^1 + \xi\mathbf{r}_y^2$, where the superscript refers to the node number, then $\mathbf{r}_{xy} = (1/l)(\mathbf{r}_y^2 - \mathbf{r}_y^1)$, which shows that $\mathbf{r}_{xy}$ does not change within the element. The linear interpolation ensures that the cross-section remains planar (no warping); an assumption required for the discussion presented in this section.

5. Using the assumption that $\mathbf{r}_y = \begin{bmatrix} -\sin\theta_c & \cos\theta_c \end{bmatrix}^T$, one can show that the material curvature matrix $\boldsymbol{\kappa}$, in this case, is defined by Eq. 21, where s is the arc length and $\theta_c' = \partial\theta_c / \partial s$. As demonstrated in this section, counter examples can be developed to demonstrate that the material curvature matrix is not related to curvature.

6. The material curvature matrix $\boldsymbol{\kappa}$ used by some researchers in the mechanics community is not related to the curvature matrix $\boldsymbol{\kappa}_f$ used in differential geometry. In some ANCF investigations [36], the tangent and cross section frames were used to define geometric parameters. Using these two different frames, two different definitions for the matrix $\boldsymbol{\kappa} = \mathbf{R}^T \left(\partial \mathbf{R} / \partial s \right)$ were provided. It is important, however, to emphasize the following facts: (1) when ANCF finite elements are used, the skew-symmetric matrix $\boldsymbol{\kappa} = \mathbf{R}^T \left(\partial \mathbf{R} / \partial s \right)$ converges to the Serret-Frenet skew-symmetric matrix in the case of small shear. This is not the case when LRVF finite elements are used because of the use of independent interpolation for the finite rotations; (2) As stated in a previous publication [36, p. 1138 with reference to Eq. 49] "*Using the assumption that the longitudinal axis of the cross-section frame does not significantly differ from the tangent to the beam centerline,* $\bar{\boldsymbol{\kappa}}_1$ *in the preceding equation can be assumed to represent the torsion. One, however, must ensure that the definition of torsion is correctly interpreted when the cross-section frame is used, particularly in the case of large deformation problems*", which implies that if the normal to the cross section is aligned with the tangent vector, different ANCF frames will lead to the same definitions of $\boldsymbol{\kappa} = \mathbf{R}^T \left(\partial \mathbf{R} / \partial s \right)$ and such definitions converge to the Serret-Frenet skew-symmetric matrix definition; (3) The ANCF tangent frame leads to the same curvature definition as the Serret-Frenet frame definition in the planar and spatial cases; and (4) In general and in the case of large shear deformations, the

ANCF cross-section frame should not be used to define any curvature matrix since in this case the matrix $\boldsymbol{\kappa} = \mathbf{R}^T \left(\partial \mathbf{R} / \partial s \right)$ does not represent correctly the zero bending in the SWB case.

5. Numerical results

Two simple numerical examples are used in this section to examine the value of the curvature obtained using two distinctly different approaches: differential geometry-based curvature (referred to in the result figures as *geometrically correct*) and cross-section-based material curvature. The differential geometry based curvature refers to $\kappa = \left| \mathbf{r}_{ss} \right|$, whereas the material curvature refers to Eq. 21. The two-dimensional shear deformable ANCF fully-parameterized beam element is used to obtain the numerical results in the examples considered in this section.

5.1 S*hear deformation without bending*

In the SWB example considered in this section, a set of prescribed nodal coordinates, as defined by Eq. 8, is used for the beam mesh and the curvature measures are evaluated in order to study their relevance in this SWB mode. For this case, the following data are used: $x_1 = y_1 = 0$, $\theta = 0°$, $l = 2\text{m}$, $t = 0.5\text{m}$ and $\gamma_1 = -\gamma_2 = 45°$. This deformation mode is shown for a mesh of 1 element and 1000 elements in Fig. 6 and Fig. 7, respectively. It can be seen from Figs. 6 - 7 that the centerline remains un-deformed in this mode of deformation demonstrating the fact that this is not a bending mode of deformation. Figure 8 compares the geometrically correct differential geometry-based curvature and the material curvature as a function of the beam arc-length for the 1 element mesh. It is clear from Fig. 8 that the geometrically correct curvature is zero along the beam arc-length while the material curvature is non-zero. The results of this figure show that the bending strain energy, if evaluated using the material curvature definition, is non-zero in the SWB case. Figure 9 compares the two different curvature measures for the 1000 element mesh. It can

be seen from Fig. 9 that the material curvature value has converged to approximately 0.785 due to mesh refinement that reduces errors due to FE-interpolation while the geometrically correct curvature remains zero. Furthermore, in order to explain analytically and confirm the results of the geometrically correct curvature definition that the deformation considered in this example is not associated with bending, the nodal coordinate vector of the 1 element mesh given by Eq. 8 is substituted in the element displacement field $\mathbf{r} = \mathbf{S}\mathbf{e}$. In this special case, $\bar{\mathbf{r}}_x = \begin{bmatrix} 1 & 0 \end{bmatrix}^T$ and $\bar{\mathbf{r}}_{xx} = \mathbf{0}$. Using Eq. 7, $\mathbf{r}(x,y,t) = \bar{\mathbf{r}}(x,t) + y\mathbf{r}_y(x,t)$, and the fact that for this element $\left(\partial \mathbf{r}_{yx} / \partial x\right) = \mathbf{0}$, one can show that $\mathbf{r}_{xx} = \mathbf{0}$ everywhere in the element, proving that the SWB case does not produce bending, and the two deformation modes are indeed kinematically independent. Based on this simple analysis, an explanation for the curved geometry on the upper and lower boundaries when 1000 elements are used (Fig. 7) can be provided. We note that continuity on the gradients and curvatures are not enforced at material points away from the beam center line. It follows that when $\gamma_1 = -\gamma_2$, $\mathbf{r}_x(x,y,t) = \bar{\mathbf{r}}_x(x,t) + y\mathbf{r}_{xy}(x,t)$ at an arbitrary point on the element remains parallel to $\bar{\mathbf{r}}_x$ as evident by the results of the single element mesh presented in Fig. 6. When more than one element is used and only γ_1 and γ_2 are prescribed at the end nodes of the beam (not for each element) such that $\gamma_1 = -\gamma_2$, $\mathbf{r}_x$, in general, does not remain parallel to $\bar{\mathbf{r}}_x$ because of the FE approximation which leads to different shear angles at the interior nodes. This explains the results of Fig. 7 despite the fact that the condition $\mathbf{r}_{xx} = \mathbf{0}$ remains in effect because $\mathbf{r}_{xy}$ remains constant within each element in the mesh, leading to zero curvature in the example considered in this section.

5.2 *Bending deformation without shear*

The second numerical example considered is that of 'inextensible' bending deformation without shear. This BWS deformation mode is achieved by starting with a straight undeformed beam, and applying simply supported boundary conditions to the beam structure and equal and opposite moments at the two ends of the beam. The beam properties considered in this example are given as follows: $l = 2\text{m}$, $h = 0.5\,\text{m}$, $t = 0.1\text{m}$, $E = 2\times10^{6}\,\text{Pa}$ and $\nu = 0$. The moment is selected to be $M = 1000\text{N.m}$. The general continuum mechanics approach with a plane stress assumption is used to obtain the solution to the static problem, and the curvature measures are evaluated using the obtained static solution. The y deformation for 1 and 1000 element meshes is shown in Figs. 10 and 11 respectively. Figures 12 and 13 show the curvature field along the beam centerline as a function of the beam arc-length for the 1 and 1000 element meshes, respectively. There is a difference in the curvature distribution when the two curvature measures are used with the 1 element mesh. Even though this mesh is considered too coarse to be used for practical problems, the values of both the curvature measures are within a small range of each other. As can be seen from Fig. 13, which shows the distribution of the curvature measures in the 1000 element mesh, both the geometrically-correct and material curvature definitions yield the same result. The reason for this is that in this specific BWS case, the beam shear angle is zero. Since the cross-section angle can be written as the sum of the rotation due to bending deformation (i.e. rotation of the normal to centerline) and rotation due to shear angle, and since the shear angle is zero, the material curvature is dependent on the centerline rotation and yields the same results as that of the geometrically-correct curvature. These results show that the material curvature converges to the geometrically correct curvature only when the shear deformation is not considered.

6. Discussion

In this section, explanation and justification of the mathematical modeling, numerical discretization, order of interpolation, and curvature and shear definitions used in this paper are provided.

6.1 *Mathematical modeling and discretization procedures*

Two mathematical curvature models are used in the planar analysis considered this study. The first is the differential geometry definition which is obtained from the norm of the curvature vector defined as the second derivative of the curve position equation with respect to its arc length. The second mathematical curvature model is the one provided by Simo [15] in which the curvature is defined as the derivative of the cross section angle with respect to the arc length. This angle defines the cross section orientation in the inertial frame [15, Page 851, Section 3.1 text after Eq. 3.1a]. The use of the relative angles will require in general the definition of the Serret-Frenet frame transformation and use this transformation with the transformation matrix that defines the orientation of the cross section to define the relative angles. This can lead to a very complex expression and can significantly increase the degree of nonlinearity. This approach was not followed in [15] to determine the shear or the curvature. Since an absolute and not a relative angle was used in the second mathematical model of the curvature [15], such an angle also includes the shear effect, and therefore, shear will possibly contribute to the curvature definition. Nonetheless, the shear, as defined in the Timoshenko's beam theory, is measured as the angle between the cross section and the normal to the beam centerline. This angle in the classical shear definition is assumed to be independent from the angle that defines the orientation of the normal to the centerline. When formulating the stress forces, Timoshenko's shear definition should be considered as an approximation when compared to the more general continuum mechanics shear definition.

The mathematical definition of the shear adopted in this paper is the basic continuum-mechanics definition. The shear strain is defined in terms of the dot product of two gradient vectors. This continuum mechanics definition clearly shows that the shear is zero and is not affected by the stretch as long as the two gradient vectors are orthogonal. If the gradient vectors are not orthogonal, the stretch will also contribute to the change in the shear strain even in the case in which the angle between the gradient vectors do not change.

The above brief introduction explains the mathematical models used in this paper. In order to examine these models, *numerical discretization* is used in this study. To this end, a fully-parameterized ANCF planar beam element is used. The goal is not to perform a convergence study, but rather to use this simple element to shed light on the definition of shear and bending considered in this investigation. A more detailed convergence study focused on the curvature definition is provided in [37]. The results presented in the literature also show that the use of the derivative of the angle that defines the orientation of the cross section to define the curvature can lead to wrong solutions when the shear is dominant [37].

6.2 *Interpolation order and curvature definitions*

It is also important to note thatThere are several planar ANCF beam elements that have varying orders of assumed displacement field interpolation in the beam longitudinal and transverse directions. The original ANCF beam element proposed by Omar and Shabana [20] is cubic in the longitudinal beam parameter and linear in the transverse parameter. The shape functions of this element are provided in Appendix A. The quadratic and the linear planar ANCF beam elements proposed by Nachbagauer [21] have quadratic and linear interpolation in the beam longitudinal direction respectively and linear interpolation in the beam transverse direction.

The third order interpolation in the beam longitudinal direction yields a linear curvature field when the geometrically correct curvature is used. As mentioned previously, linear and quadratic longitudinal beam interpolations lead to zero and constant curvature fields within the element. The partial differential equation that governs the vibration of beams has fourth order partial derivative with respect the beam spatial coordinate. This order of derivative ensures that that assumed displacement field or the eigen functions obtained from the classical solution of the bending vibration problem do not produce zero or constant curvature. In the conventional FE approach, this requirement, for the most part, has been observed when developing beam and plate elements. Conventional beam elements that employ infinitesimal rotations are based on cubic interpolation for the transverse deformation. This requirement is also ensured when using the ANCF element considered in this study. The element is based on a cubic interpolation in the longitudinal direction. When lower-order of interpolations is used, accurate definition of the curvature can be difficult to obtain. For example, in [15], linear interpolation was used, and as a consequence, the curvature is zero within the element. Furthermore, when lower order elements are used, a finer mesh will be required compared to higher order elements, due to the deficiency in correctly capturing the curvature field. Moreover, several locking phenomena might exist in lower order elements that will require dealing with in addition to using a finer mesh. However, on a more fundamental note, zero and constant element curvature fields can be more important issues as compared to mesh size and locking issues. Additionally, higher order elements can also assist in better capturing the geometry being analyzed while using a much smaller mesh.

7. Summary and conclusions

This paper is concerned with the interpretation of the geometric invariants, such as the curvature, in the FE large displacement analysis. This study is motivated by the fact that the definition of curve and surface invariants is fundamental for the accurate formulation of the stress forces in beam and plate problems, particularly in the case of large displacement analysis. The fact that shear and bending are independent modes of deformation implies that there is no kinematic coupling between these two modes despite the fact that kinetic coupling may exist. Using simple examples, the paper clearly demonstrates how higher-order finite elements can be used to obtain, at an arbitrary point and along a certain direction, shear without bending and bending without shear. Such a demonstration is necessary in order to shed light on some of the curvature definitions used in computational mechanics. The FE representation of the two kinematically-uncoupled modes of deformation (shear and bending) was evaluated in order to examine the effect of the order of the polynomial interpolation on the accuracy of representing these two independent modes. It is also demonstrated that not all the curvature vectors contribute to bending deformation. Curvature vectors that define the change of the orientation of vectors tangent to a coordinate line along the same coordinate line contribute to bending. The analysis presented in this paper is used to shed light on the definition of the *material curvature* used in the literature. The problems associated with the use of the material curvature matrix, obtained using the rotation of the beam cross-section, are discussed. The fundamental differences between the material curvature and the Serret-Frenet curvature are also highlighted. The results obtained in this investigation show that the material curvature definition can lead to significant errors when shear is dominant, and the material curvature converges to the geometrically correct curvature only when the shear deformation is not considered. This paper is focused on the planar case in order to avoid the

complexities of the three-dimensional analysis which will be considered in future investigations aimed at extending and generalizing the conclusions drawn from this study.

Appendix

The displacement field of the planar shear-deformable ANCF element used in this investigation can be written as $\mathbf{r} = \mathbf{S}\mathbf{e}$, where $\mathbf{r}$ is the global position vector of an arbitrary point on the element, $\mathbf{S}$ is the element shape function matrix, and $\mathbf{e}$ is the vector of the element nodal coordinates defined as $\mathbf{e} = \begin{bmatrix} \mathbf{r}^{1T} & \mathbf{r}_x^{1T} & \mathbf{r}_y^{1T} & \mathbf{r}^{2T} & \mathbf{r}_x^{2T} & \mathbf{r}_y^{2T} \end{bmatrix}^T$, where superscripts refer to the node number. The shape function matrix $\mathbf{S}$ is defined as

$$\mathbf{S} = \begin{bmatrix} s_1 & 0 & s_2 & 0 & s_3 & 0 & s_4 & 0 & s_5 & 0 & s_6 & 0 \\ 0 & s_1 & 0 & s_2 & 0 & s_3 & 0 & s_4 & 0 & s_5 & 0 & s_6 \end{bmatrix} \tag{A.1}$$

where the functions $s_i = s_i(\xi, \eta)$ are defined as

$$\left.\begin{aligned} s_1 &= 1 - 3\xi^2 + 2\xi^3, \quad s_2 = l\left(\xi - 2\xi^2 + \xi^3\right), \quad s_3 = \eta l\left(1 - \xi\right), \\ s_4 &= 3\xi^2 - 2\xi^3, \quad s_5 = l\left(-\xi^2 + \xi^3\right), \quad s_6 = \xi\eta l \end{aligned}\right\} \tag{A.2}$$

References

1. J. Bonet, R.D. Wood, Nonlinear Continuum Mechanics for Finite Element Analysis, Cambridge University Press, Cambridge, 1997.
2. R.W. Ogden, Non-Linear Elastic Deformations, Ellis Harwood Ltd., Chichester. 1984.
3. A.A. Shabana, Computational Continuum Mechanics, third ed., Cambridge University Press, Cambridge, 2017.
4. P. Dierckx, Curve and Surface Fitting with Splines, Oxford University Press, New York, 1993.
5. G. Farin, Curved and Surfaces for CAGD, A Practical Guide, fifth ed., Morgan Kaufmann Publishers, San Francisco, 1999.
6. E. Kreyszig, Differential Geometry, Dover Publications, New York, 1991.
7. L. Peigl, W. Tiller, The NURBS Book, second ed., Springer-Verlag, New York, 1997.
8. S.S. Antman, The theory of rods, Handbuch der Physics VIa/2 (1972) 641-703.
9. S.S. Antman, Kirchhoff's problem for nonlinearly elastic rods, Quarterly of Applied Mathematics 32 (1974) 221-240.
10. E. Reissner, On a one dimensional finite strain beam: the plane problem, Journal of Applied Mathematics and Physics 23 (1972) 795-804.
11. E. Reissner, On a one dimensional large-displacement finite strain beam theory, Studies in Applied Mathematics 52 (1973) 87-95.
12. E. Reissner, On finite deformations of space-curved beams, Journal of Applied Mathematics and Physics (ZAMP) 32 (1981) 734-744.
13. J.C. Simo, A finite strain beam formulation. The three dimensional dynamics problem. Part I, Computer Methods in Applied Mechanics and Engineering 49 (1985) 55-70.

14. J.C. Simo, L. Vu-Quoc, A three-dimensional finite-strain rod model, Part II: Computational aspects, Computer Methods in Applied Mechanics and Engineering 58 (1986A) 79-116.
15. J.C. Simo, L. Vu-Quoc, On the dynamics of flexible beams under large overall motions-the plane case: Parts I and II, ASME Journal of Applied Mechanics 53 (1986B) 849-863.
16. J. Ding, M. Wallin, C. Wei, A. Recuero, A.A. Shabana, Use of independent rotation field in the large displacement analysis of beams, Nonlinear Dynamics 76 (2014) 1829-1843.
17. O. Dmitrochenko, A. Mikkola, Digital nomenclature code for topology and kinematics of finite elements based on the absolute nodal coordinate formulation, IMechE Journal of Multibody Dynamics 225 (2011) 34-51.
18. W. Hu, Q. Tian, H.Y. Hu, Dynamics simulation of the liquid-filled flexible multibody system via the absolute nodal coordinate formulation and the SPH method, Nonlinear Dynamics 75 (2014) 653-671.
19. C. Liu, Q. Tian, H.Y. Hu, Dynamics of large scale rigid-flexible multibody system composed of composite laminated plates, Multibody System Dynamics 26 (2011) 283-305.
20. M.A. Omar, A.A. Shabana, A two-dimensional shear deformable beam for large rotation and deformation problems, Sound Vibration 243 (2001) 565-576.
21. K. Nachbagauer, Development of shear and cross-section deformable beam finite elements applied to large deformation and the dynamics problems, Ph.D. dissertation, Johannes Kepler University, Linz, Austria.
22. G. Orzechowski, J. Fraczek, Analysis of beam elements of circular cross-section using the absolute nodal coordinate formulation, Archive in Mechanical Engineering 59 (2012) 283-296.
23. G. Orzechowski, J. Fraczek, Integration of the equations of motion of the multibody systems using absolute nodal coordinate formulation, Acta Mechanica et Automatica 6 (2012) 75-83.

24. G. Orzechowski, J. Fraczek, Nearly incompressible nonlinear material models in the large deformation analysis of beams using ANCF, Nonlinear Dynamics 82 (2015) 451-464.
25. A.A. Shabana, ANCF consistent rotation-based finite element formulation, ASME J. Comp. Nonlinear Dynamics 11 (2016) (ID 014502).
26. Q. Tian, L.P. Chen, Y.Q. Zhang, J.Z. Yang, An efficient hybrid method for multibody dynamics simulation based on absolute nodal coordinate formulation, ASME Journal of Computational and Nonlinear Dynamics 4 (2009) (ID 021009).
27. Q. Tian, Y.L. Sun, C. Liu, H.Y. Hu, F. Paulo, Elasto-hydro-dynamic lubricated cylindrical joints for rigid-flexible multibody dynamics, Computers & Stuctures 114-115 (2013) 106-120.
28. W.S. Yoo, J.H. Lee, S.J. Park, J.H. Sohn, D. Pogorelov, O. Dimitrochenko, Large deflection analysis of a thin plate: Computer simulation and experiment, Multibody System Dynamics. 11 (2004) 185-208.
29. Y. Zheng, A.A. Shabana, A two-dimensional shear deformable ANCF consistent rotation-based formulation beam element, Nonlinear Dynamics 87 (2015) 1031-1043.
30. K.J. Bathe, Finite Element Procedures, Prentice Hall Inc., Englewood Cliffs, 1996.
31. R.D. Cook, D.S. Malkus, M.E. Plesha, Concepts and Applications of Finite Element Analysis, third ed., John Wiley and Sons, New York, 1989.
32. M.A. Crisfield, Nonlinear Finite Element Analysis of Solids and Structures Vol. 1: Essentials, John Wiley and Sons, New York, 1991.
33. H. Goldstein, Classical Mechanics, first ed., Addison Wesley, Massachusetts, 1950.
34. R.E. Roberson, R. Schwertassek, Dynamics of multibody systems, first ed., Springer-Verlag, Berlin, 1988.
35. A.A. Shabana, Computational Dynamics, third ed., John Wiley and Sons, New York, 2010.

36. H. Sugiyama, J. Gerstmayr, A.A. Shabana, Deformation modes in the finite element absolute nodal coordinate formulation, Sound and Vibration 298 (2006) 1129-1149.

37. Y. Zheng, A.A. Shabana, A.A., D. Zhang, Curvature expressions for the large displacement analysis of planar beam motions, *ASME Journal of Computational and Nonlinear Dynamics*, accepted for publication.

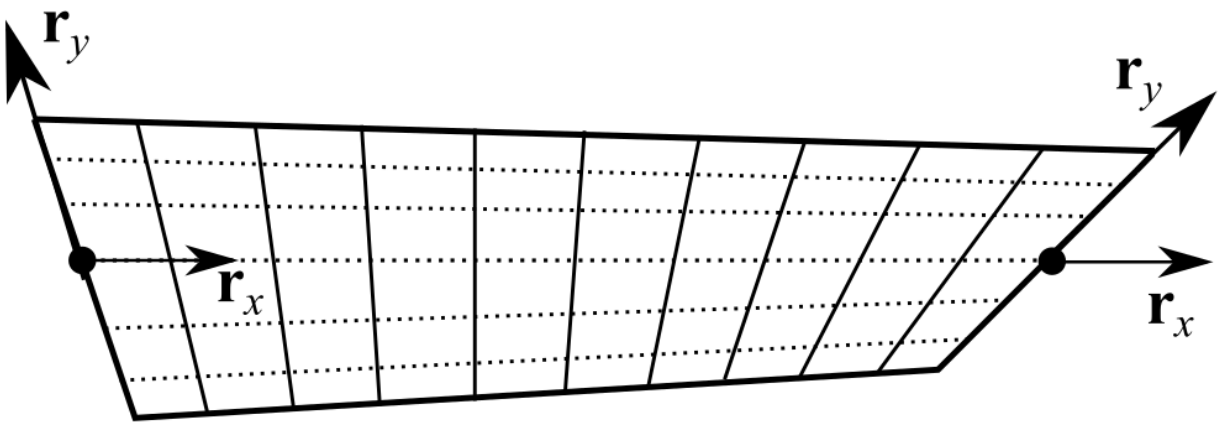

Figure 1. Non-uniform shear deformation using the elements of Ref. 20 (▪▪▪▪▪▪▪▪ x coordinate lines; ——— y coordinate lines)

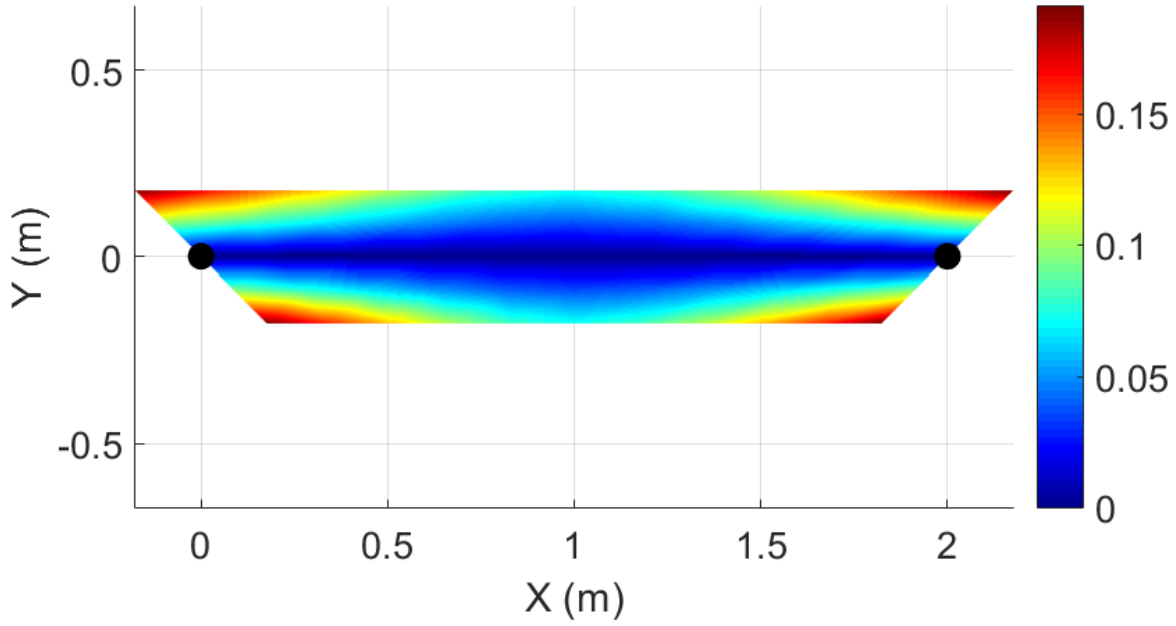

Figure 2. Total deformation contours in the SWB example defined by Eq. 8 for $\gamma_1 = 45°$ and $\gamma_2 = -45°$

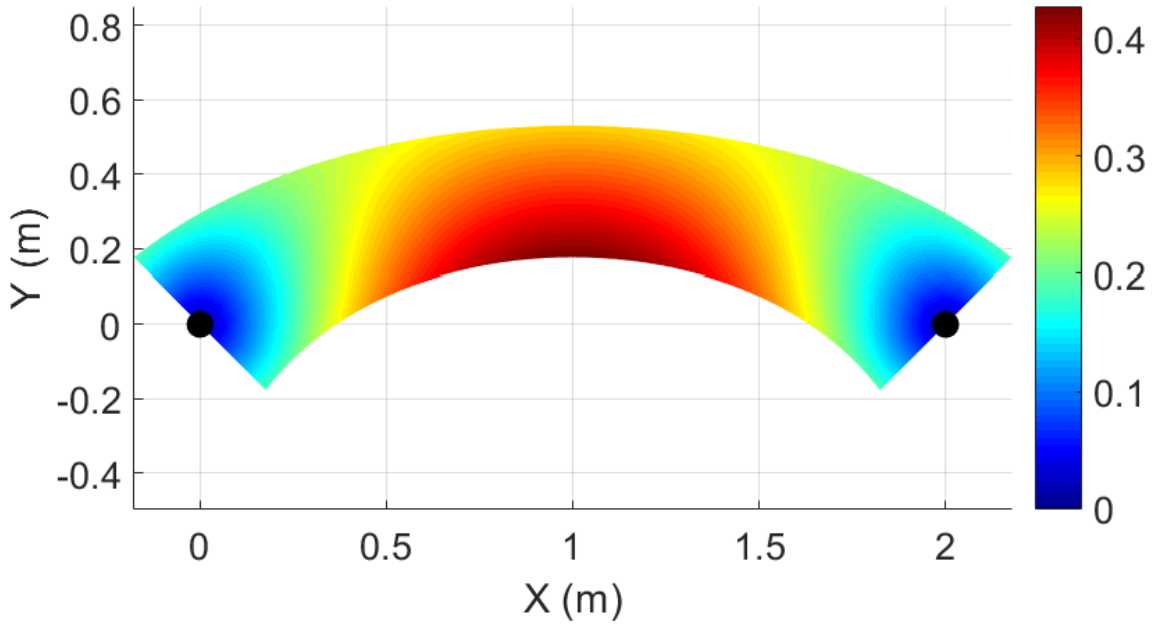

Figure 3. Total deformation contours in the bending example defined by Eq. 12 for $\beta_1 = 45°$ and $\beta_2 = -45°$

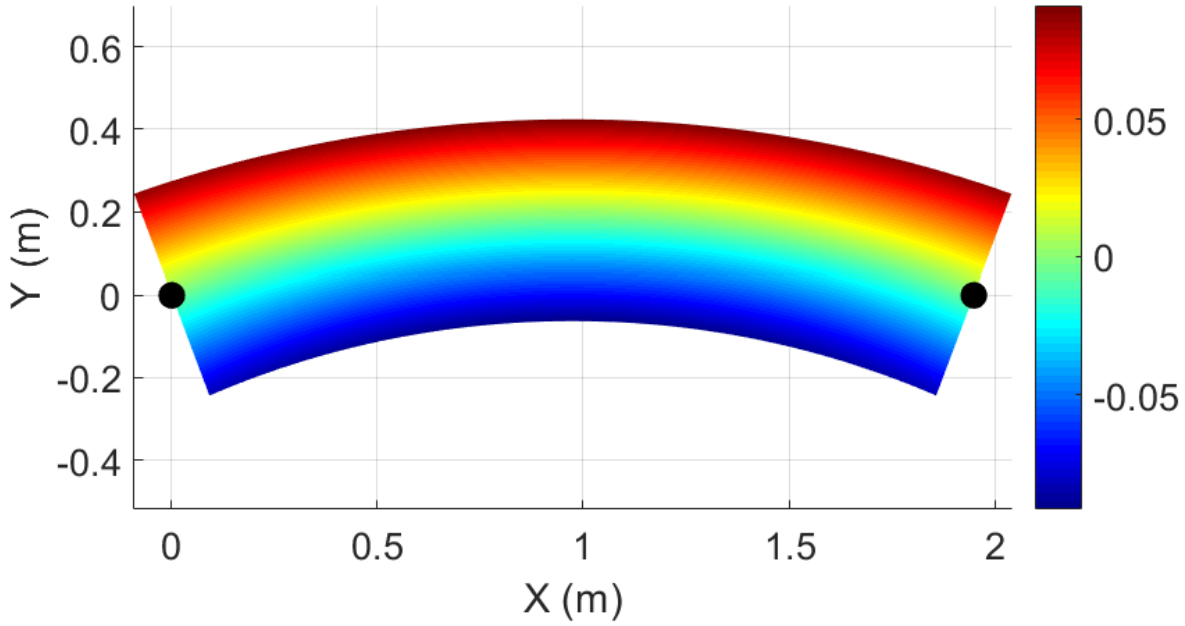

Figure 4. Axial strain contours in symmetric bending without shear

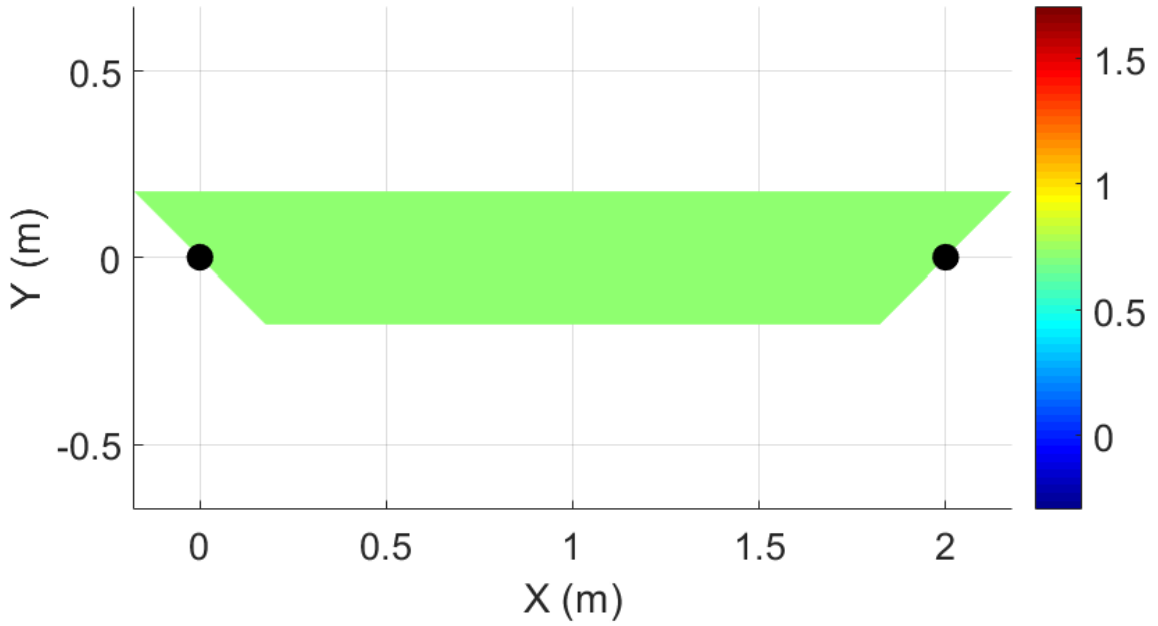

Figure 5. Constant $\left|\mathbf{r}_{yx}\right|$ contours in the SWB example defined by Eq. 8 for $\gamma_1 = 45°$ and $\gamma_2 = -45°$

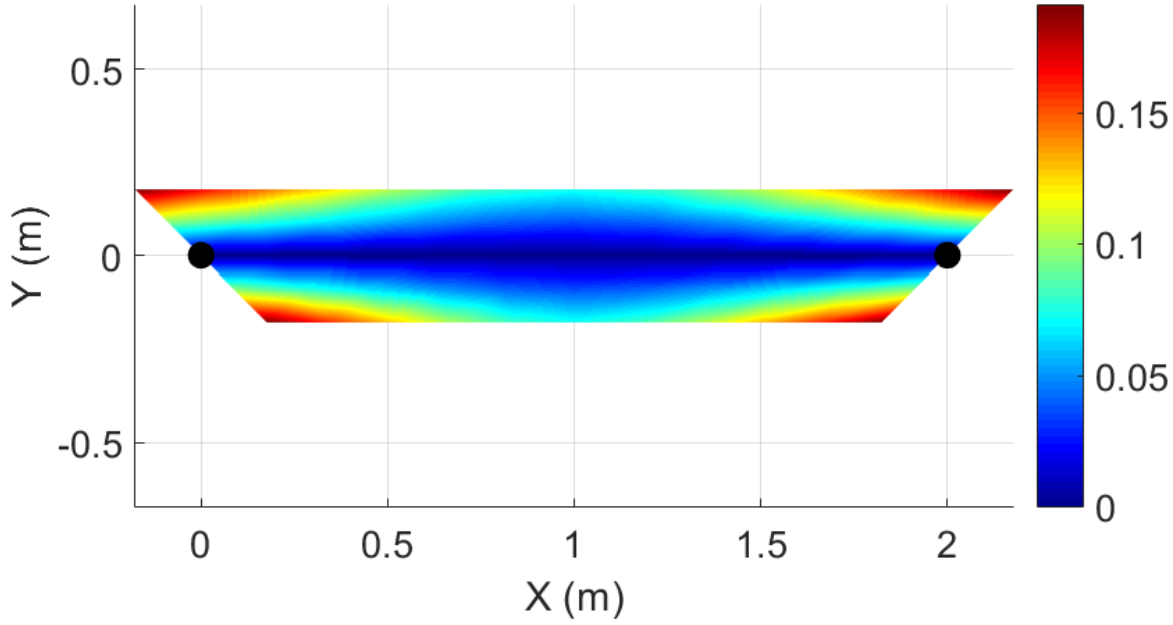

Figure 6. Total deformation contours in 1 element mesh in the SWB case

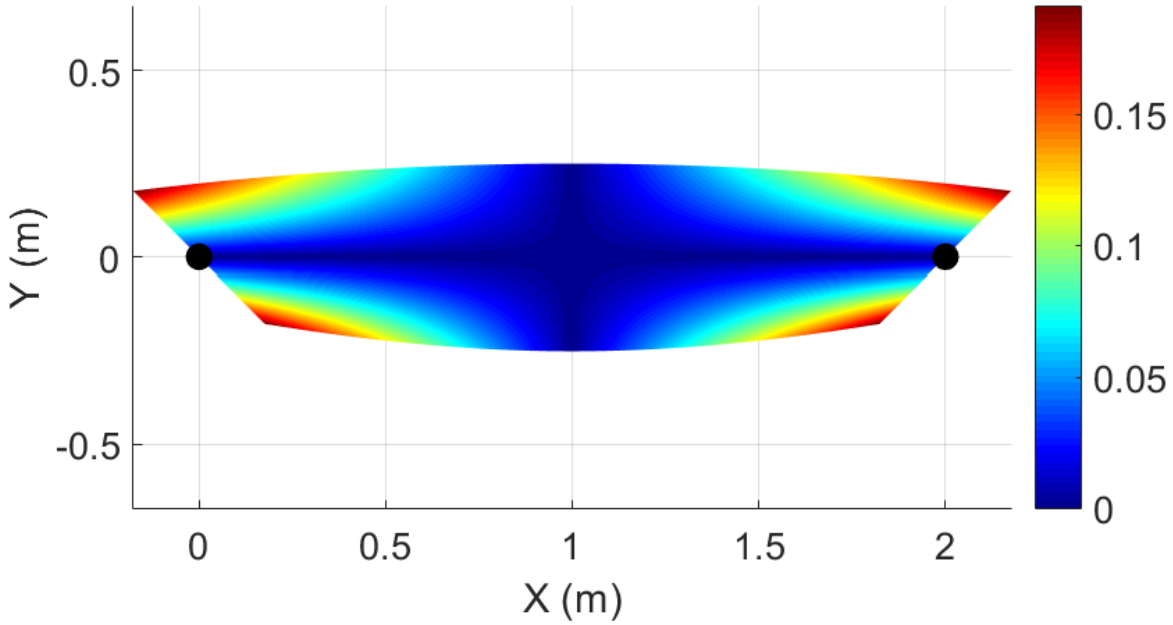

Figure 7. Total deformation contours in 1000 element mesh in the SWB case

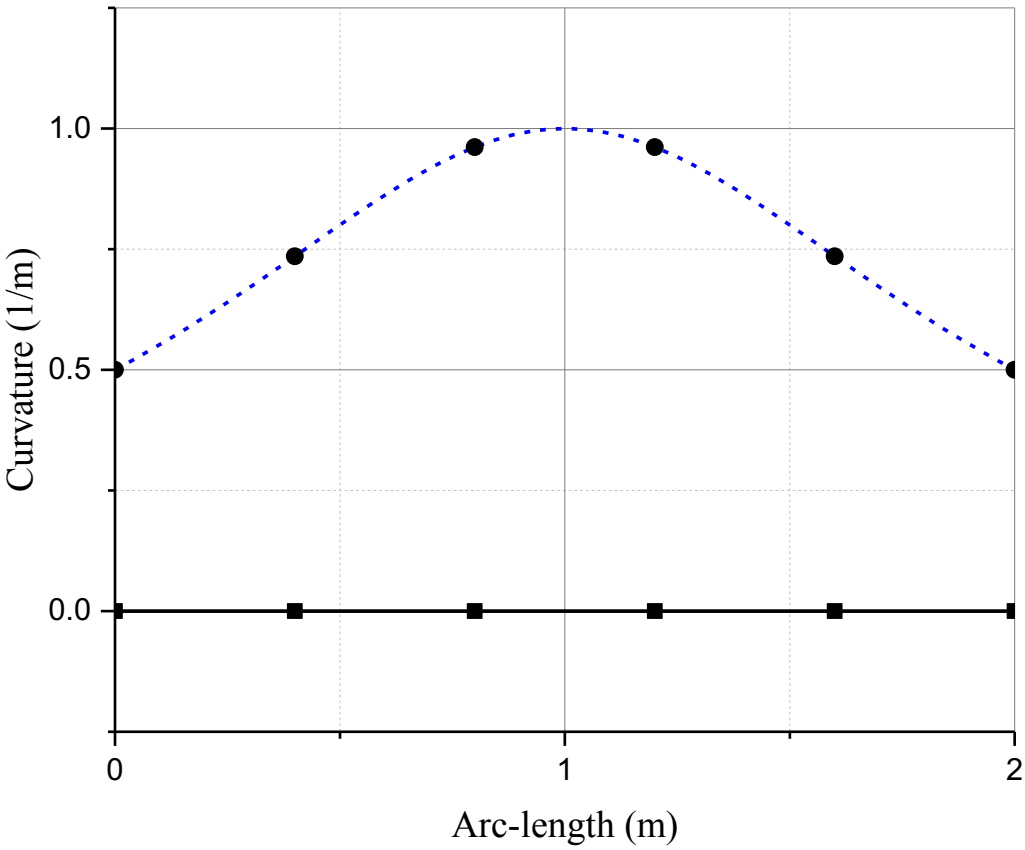

Figure 8. Comparison of curvature measures in 1 element mesh in the SWB case

(Geometrically correct curvature; Material curvature)

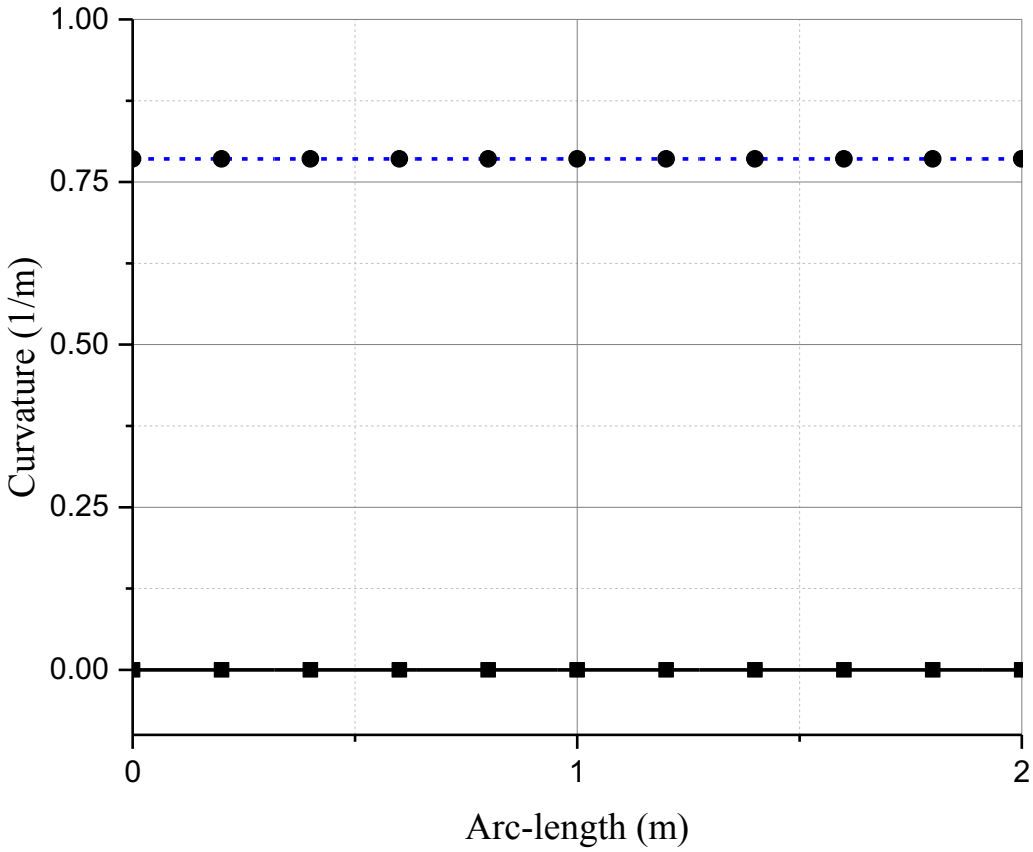

Figure 9. Comparison of curvature measures in 1000 element mesh in the SWB case

(Geometrically correct curvature; Material curvature)

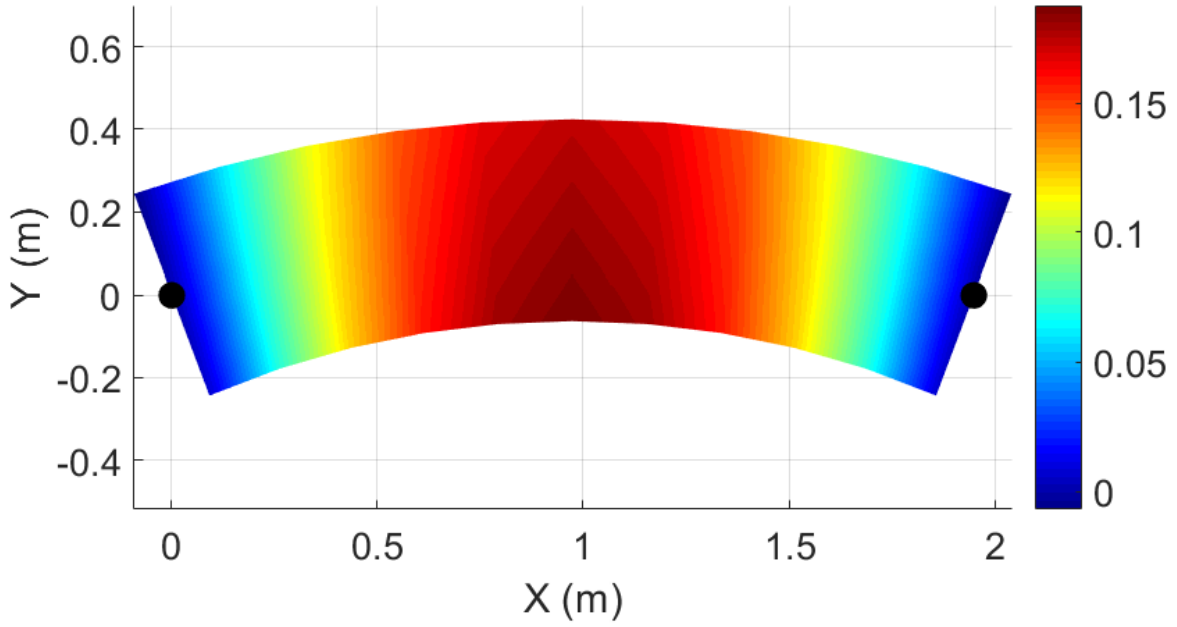

Figure 10. *y* deformation contours in 1 element mesh in the BWS case

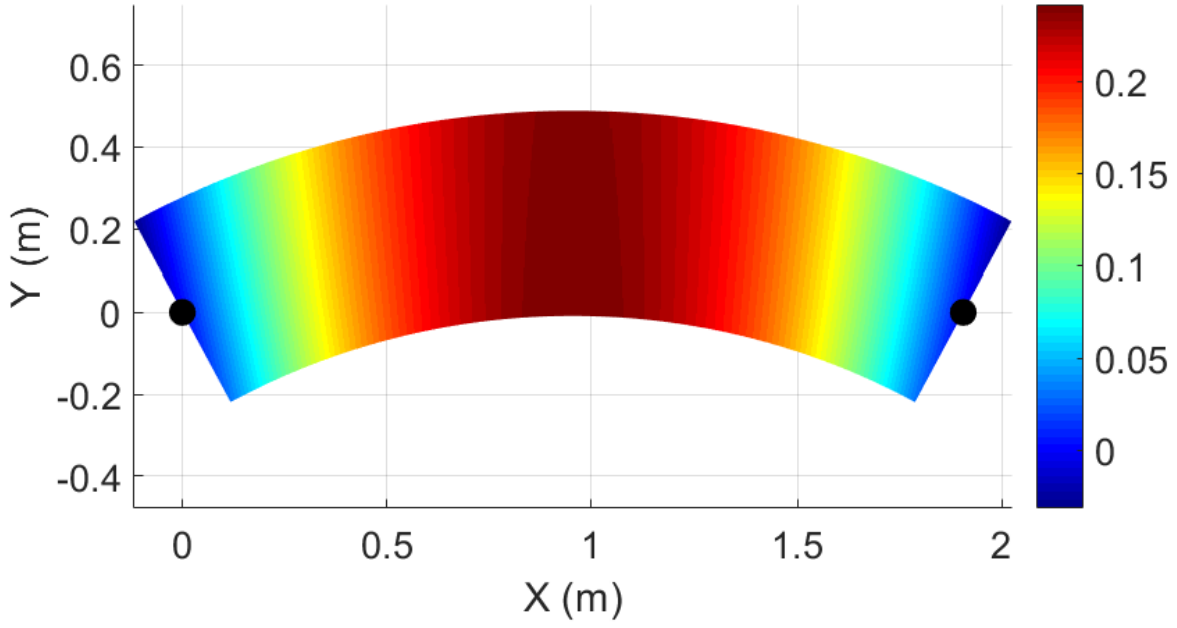

Figure 11. *y* deformation contours in 1000 element mesh the BWS case

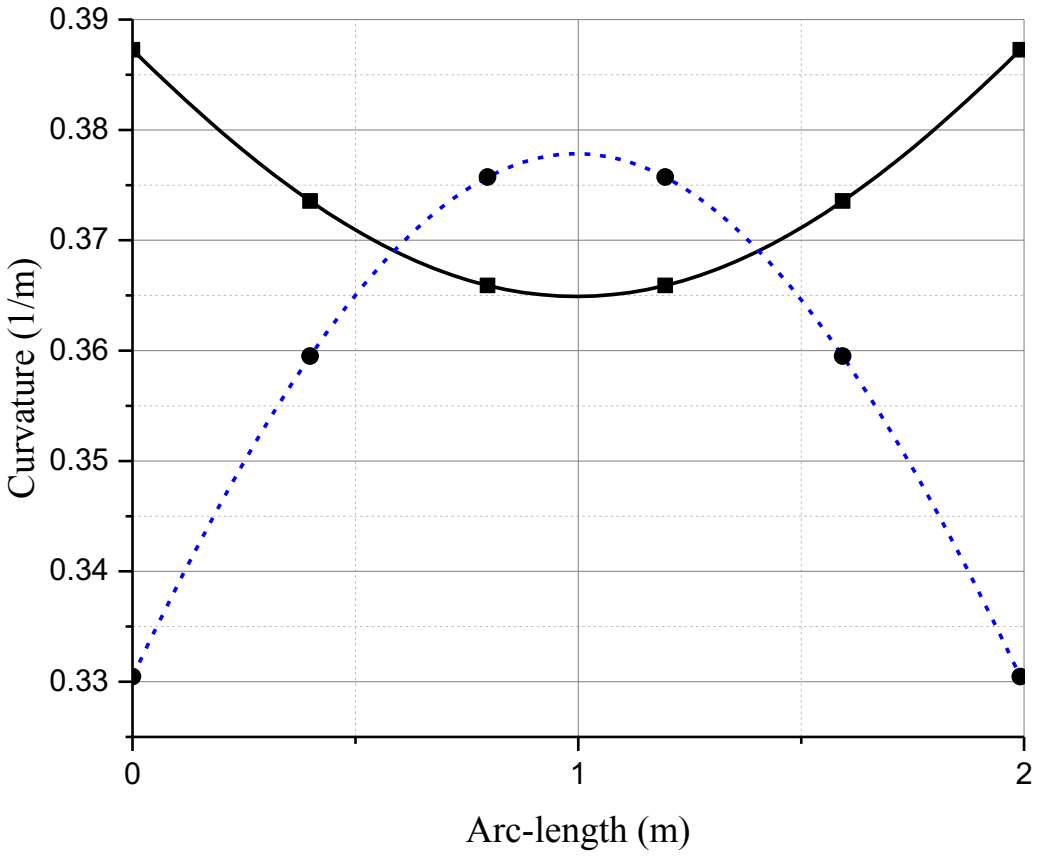

Figure 12. Comparison of curvature measures in 1 element mesh in the BWS case

(Geometrically correct curvature; Material curvature)

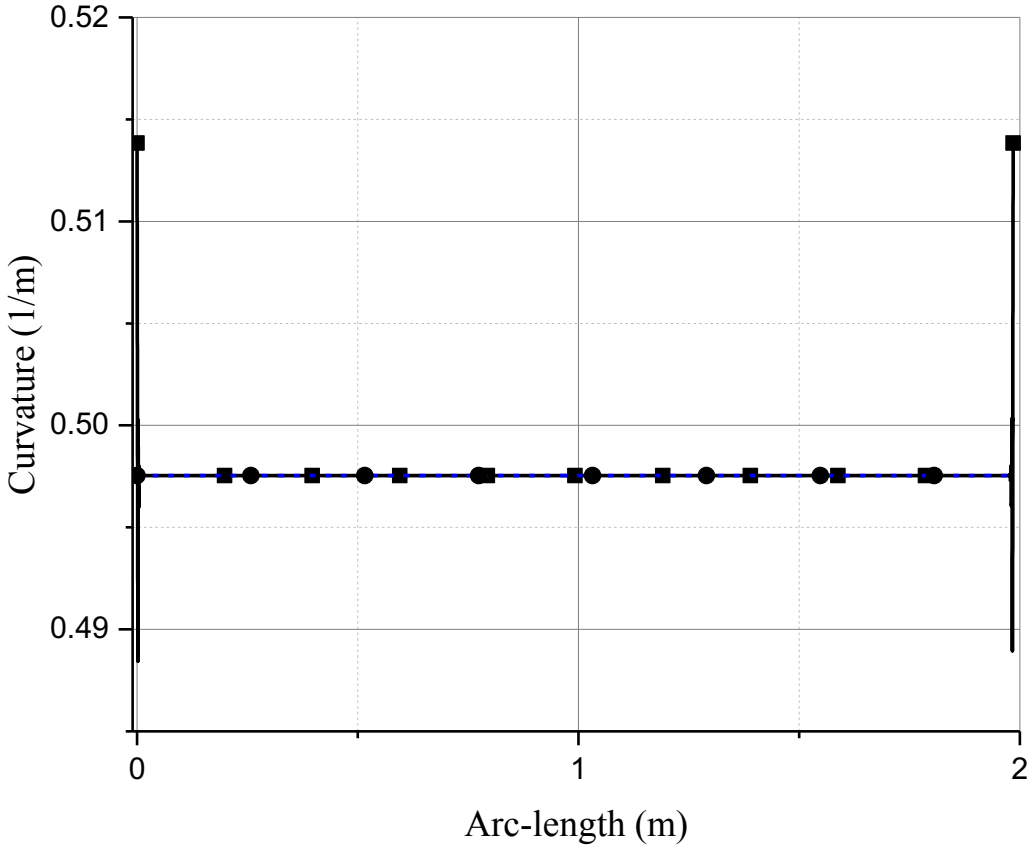

Figure 13. Comparison of curvature measures in 1000 element mesh in the BWS case (—■— Geometrically correct curvature; - - -●- - - Material curvature)